© 2020. Published by The Company of Biologists Ltd | Development (2020) 147, dev183715. doi:10.1242/dev.183715

RESEARCH REPORT

Arabidopsis DIACYLGLYCEROL KINASE4 is involved in nitric oxide-dependent pollen tube guidance and fertilization

Aloysius Wong[1,2], Lara Donaldson[2,3], Maria Teresa Portes[4], Jörg Eppinger[5], José A. Feijó[4,*] and Christoph Gehring[2]

ABSTRACT

Nitric oxide (NO) is a key signaling molecule that regulates diverse biological processes in both animals and plants, including important roles in male gamete physiology. In plants, NO is generated in pollen tubes (PTs) and affects intracellular responses through the modulation of Ca^{2+} signaling, actin organization, vesicle trafficking and cell wall deposition, bearing consequences in pollen-stigma interactions and PT guidance. In contrast, the NO-responsive proteins that mediate these responses remain elusive. Here, we show that PTs of *Arabidopsis thaliana* mutants impaired in the pollen-specific DIACYLGLYCEROL KINASE4 (DGK4) grow slower and become partially insensitive to NO-dependent growth inhibition and re-orientation responses. Recombinant DGK4 protein yields NO-responsive spectral and catalytic changes *in vitro* that are compatible with a role in NO perception and signaling in PTs. In addition to the expected phosphatidic acid-producing kinase activity, DGK4 recombinant protein also revealed guanylyl cyclase activity, as inferred by sequence analysis. Our results are compatible with a role for the fast-diffusible NO gas in signaling and cell-cell communication via the modulation of DGK4 activity during the progamic phase of angiosperm reproduction.

KEY WORDS: DGK4, Pollen tube, Nitric oxide, Fertilization, Plant sexual reproduction, H-NOX, *Arabidopsis*

INTRODUCTION

Nitric oxide (NO) is a key signaling molecule that regulates diverse biological processes in animals and plants (Wendehenne et al., 2001; Lamattina et al., 2003). In animals, NO regulates vascular wall tone, neurotransmission and immune response, whereas in plants, NO is essential for development and for responses to biotic and abiotic stresses (Wendehenne et al., 2001; Domingos et al., 2015; Astier et al., 2019). Interestingly, NO is involved in the sexual reproduction of both animals and plants, mediating events related to the male gamete physiology. In animals, NO stimulates sperm motility (Miraglia et al., 2011) and binding to the plasma membrane of oocytes (Sengoku et al., 1998), whereas in plants, NO mediates pollen-stigma interactions and pollen tube (PT) guidance (McInnis et al., 2006; Prado et al., 2008). NO generation in PTs has been demonstrated (Prado et al., 2004) and intracellular responses to NO include modulation of cytosolic Ca^{2+} elevation (likely causal for PT growth retardation, re-orientation and re-growth), actin organization, vesicle trafficking and cell wall deposition (Prado et al., 2008; Wang et al., 2009). However, the NO-responsive proteins that mediate these responses remain unknown (Domingos et al., 2015; León and Costa-Broseta, 2019).

Previously, pollen-specific *Arabidopsis* DIACYLGLYCEROL KINASE4 (DGK4; At5g57690) has been suggested to harbor a gas-sensing region (Wong et al., 2013; Domingos et al., 2015), and the DGK family has been associated with important roles in pollen germination and growth (Potocký et al., 2014). Recently, DGK4 has been assigned signaling roles related to maintaining mechanical properties in PT growth with consequences on fertility rates (Vaz Dias et al., 2019).

Here, we have investigated the NO-dependent PT growth responses in wild-type (WT) (ecotype Col-0) and DGK4-impaired plants. We show that PTs of *Arabidopsis* impaired in the pollen-specific DGK4, grow slower and become partially insensitive to NO-dependent growth inhibition and re-orientation responses. Recombinant DGK4 yields NO-responsive spectral and catalytic changes *in vitro* that are compatible with a NO perception and signaling function in PTs. These results are discussed in the context of a role for NO, as a fast-diffusible gas, in DGK4-mediated long-range signaling and/or rapid cell-cell communication during angiosperm reproduction.

RESULTS AND DISCUSSION

DGK4 is required for NO-dependent PT growth and re-orientation responses

Homozygous *dgk4* plants with a T-DNA insertion 424 bp upstream of the *DGK4* open reading frame (*dgk4-1*; SALK_151239) were determined to have a 50% knockdown (KD) in *DGK4* expression (Fig. S1). The PTs of *dgk4-1* grow significantly slower *in vitro* compared with WT across a pH range of 6.5 to 8.5, and in both optimal and reduced Ca^{2+} media (Fig. 1A). Four hours after germination, WT PTs reached an average length of 176 µm, whereas *dgk4-1* only reached 144 µm at pH 7.5 (n>100; P<0.05). This mutant line was also reported to have PTs with altered stiffness and adhesion properties (Vaz Dias et al., 2019). When exposed to the NO donor sodium nitroprusside (SNP), both WT and the *dgk4-1* PTs show NO dose-dependent reduction of growth rates (Fig. 1B), much like those reported in *Lilium longiflorum* (Prado et al., 2004), *Paulownia tomentosa* (He et al., 2007) and *Camelia sinensis* (Wang et al., 2012). At doses of between 0 and 10 nM of SNP, the decline

[1]Department of Biology, College of Science and Technology, Wenzhou-Kean University, 88 Daxue Road, Ouhai, Wenzhou, Zhejiang Province 325060, China. [2]Division of Biological and Environmental Sciences and Engineering, 4700 King Abdullah University of Science and Technology, Thuwal 23955-6900, Saudi Arabia. [3]Department of Molecular and Cell Biology, University of Cape Town, Rondebosch 7701, South Africa. [4]Department of Cell Biology and Molecular Genetics, University of Maryland, College Park, MD 20742-5815, USA. [5]Division of Physical Sciences and Engineering, Biological and Organometallic Catalysis Laboratory, KAUST Catalysis Center, 4700 King Abdullah University of Science and Technology, Thuwal 23955-6900, Saudi Arabia.

*Author for correspondence (jfeijo@umd.edu)

A.W., 0000-0002-9105-5845; L.D., 0000-0001-5727-3155; M.T.P., 0000-0001-5668-0605; J.E., 0000-0001-7886-7059; J.A.F., 0000-0002-1100-5478; C.G., 0000-0003-2451-8755

Handling Editor: Ykä Helariutta
Received 9 August 2019; Accepted 26 February 2020

Development (2020) 147, dev183715. doi:10.1242/dev.183715

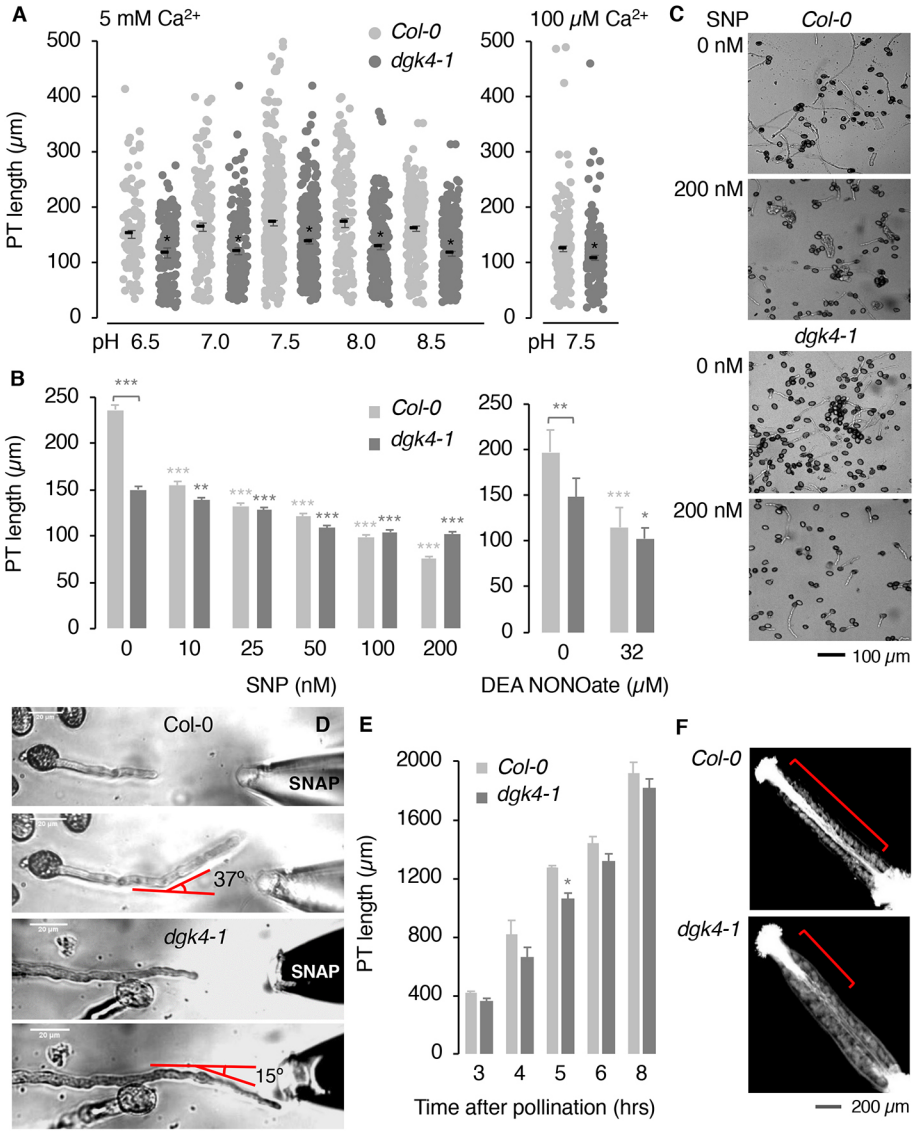

Fig. 1. *dgk4-1* PT has reduced growth and NO-dependent responses. (A) *dgk4-1* PT growth is slower than that of Col-0. This is consistent across a range of pH values (6.5-8.5), and in both optimal (5 mM) (left) and reduced (100 µM) Ca^{2+} (right) media. Data are mean±s.e.m. (n>100). *P<0.05 compared with PT length of Col-0. (B) NO-dependent inhibition of *dgk4-1* PT growth is reduced compared with Col-0. NO was provided by SNP or DEA NONOate. Data are mean±s.e.m. (n>150). *P<0.05, **P<0.005 and ***P<0.0005 compared with PT length of untreated sample. (C) Representative images of *dgk4-1* and Col-0 PTs with and without NO. (D) A representative image of the response of a growing Col-0 PT bending away from an agarified NO glass probe, containing SNAP (10 mM) at a sharper angle than *dgk4-1* (see also Fig. S3). (E) PT growth in the pistil of *dgk4-1* is slowed compared with Col-0, with the representative pistil image at 5 h postfertilization (F) showing a higher density (red bracket) of longer Col-0 PTs. Data are mean±s.e.m. (n>3). *P<0.05 compared with PT length of Col-0.

in growth rate for WT is 34.52% but, in contrast, the decline for *dgk4-1* in the same range is only 7.86%. Importantly, PTs of *dgk4-1* become insensitive to SNP concentration increases over 50 nM, whereas the rate of WT PT growth continues to decrease up to 200 nM SNP (Fig. 1B,C). Correspondingly, we also observed differential sensitivity between WT and *dgk4-1* PTs using another NO donor, diethylamine (DEA) NONOate (Fig. 1B). A second independent homozygous *dgk4* mutant plant (*dgk4-2*; SALK_145081, T-DNA insertion 268 bp upstream of the *DGK4* gene) (Fig. S1) showed similar NO insensitivity (Fig. S2). These results suggest that the effect of NO on DGK4 activity has mechanistic consequences on PT growth.

We further examined the effect of NO on the directional growth of PTs using *dgk4-1*. Our experimental set-up was based on our previous work in lily PTs (Prado et al., 2004) in which an agarified medium containing 10 mM SNAP (s-nitroso-acethilpenilcilamine; NO donor) was loaded into a pulled glass micropipette, forming a point source of NO diffusion. Assuming that the germination medium is homogenous, a gradient concentration decrease proportional to the square of the distance from the source should be formed. For lily PTs, we experimentally determined that the threshold for the negative chemotropic re-orientation response was within the range of 5-10 nM of NO (Prado et al., 2004). Here, we reproduced these experiments with *Arabidopsis*. Both WT and *dgk-4* PTs were chosen to have growth rates within a similar range (2-4 µm min^{-1}) to minimize growth rate bias to their NO response. We observed that WT and *dgk4-1* PTs showed a negative chemotropic response, bending away from the NO source, much like our previous observations in lily (Prado et al., 2004); however, of relevance, the bending angles in WT (45.8±6.3°; n=10) were twice as acute as those in *dgk4-1* (22.9±2.6°; n=10) (Fig. 1D; Fig. S3). Moreover, WT PTs showed clear, elbow-like points of inflections when approaching the critical NO concentration, a morphological feature also observed in lily (Prado et al., 2004) that corresponds to a slowdown of the growth rate, followed by turning of the PT (Movies 1,2). In contrast, *dgk4-1* PTs showed softer angles without elbow-like turns (Fig. 1D), even when challenged with much steeper and concentrated gradients of SNAP (Fig. S3). Both the germination and the re-orientation experiments clearly show a desensitization to NO, an effect that would be expected to be more pronounced if a full knockout of *dgk4-1* was available. Given that a dose of 5-10 nM is within the physiological range of NO action (Lamattina et al., 2003), our results are consistent with a signaling role for DGK4 in NO sensing.

Development (2020) 147, dev183715. doi:10.1242/dev.183715

In agreement with the *in vitro* germination phenotype, *in vivo* germinated PTs of *dgk4-1* also grew slower down the pistil than those of WT across all time points examined (Fig. 1E,F). To test whether these differential growth rates would result in outcompetition, we brushed a ∼50:50 mixture of pollen from Col-0 (rr) and *dgk4-1* (RR) onto an emasculated Col-0 flower (where *R*=resistant and *r*=susceptible), generating a Rr pollen cross onto a Col-0 female (rr). With no bias in fitness, a 1:1 ratio of kanamycin-resistant and susceptible offspring would be expected, but rather we observed a percentage of 36.3% (n=99) kanamycin-resistant offspring, revealing that WT PTs outperformed *dgk4-1* PTs. This finding is consistent with that reported for a different *dgk4* mutant allele (Vaz Dias et al., 2019).

DGK4 yields NO-responsive spectral changes and catalytic activity

We next focused on determining the molecular basis of the NO-sensing properties of DGK4. Through sequence analysis we have previously predicted that DGK4 contains a region spanning from H350 to R383, similar to heme centers of functional gas-responsive heme-NO/oxygen (H-NOX), heme-NO-binding and NO-sensing families of proteins in other kingdoms (Domingos et al., 2015; Wong et al., 2018). In particular, this region harbors the HX[12]PX[14,16]YXSXR consensus pattern derived from heme *b* containing H-NOX centers in proteins from bacteria and animals, and is present in plant orthologs, such as poplar, castor bean and soybean, but absent in other *Arabidopsis* DGKs (Fig. 2A). The presence of the H-NOX-like signature suggests that DGK4 might accommodate a heme *b* and, correspondingly, the diagnostic spectral properties should have a distinct response to NO. Recombinant DGK4 yields a Soret peak at 410 nm (Fig. 2B), which is distinctly different from unbound hemin (protohemine IX: Soret band at 435 nm with a shoulder at 400 nm) and falls within the typical peak range observed for proteins with a histidine-ligated ferric heme *b* (Walker et al., 1999). Reduction with sodium dithionite resulted in a red shift of the Soret peak to 424 nm accompanied by the emergence of distinct α (558 nm) and β (526 nm) bands (Fig. 2B; Fig. S4A). The ferrous state presumably represents the native state of DGK4 in the cytosol [*Arabidopsis* cytosolic redox potential: −310 to −240 mV (Aller et al., 2013)]. Exposure to air recovers the oxidized Soret peak (410 nm) of DGK4 after 20 min (Fig. S4A). Importantly, addition of DEA NONOate attenuates the reduced Soret absorption (424 nm) in a concentration-dependent manner, hinting at the possibility of NO displacing the histidine ligand from the heme group (Fig. 2C; Fig. S4B). This is an essential step in the signaling of canonical H-NOX proteins (Russwurm and Koesling, 2004).

Qualitatively, the spectroscopic behavior resembles that of canonical H-NOX proteins, e.g. the H-NOX domain of *Shewanella oneidensis*, which showed Soret absorptions at 403 nm (ferric), 430 nm (ferrous) and 399 nm (ferrous, NO bound) (Dai et al., 2012). However, the frequencies and relative intensities of the Soret α and β peaks are indicative of a bis-histidine ligated heme *b* center, as found in cytochromes *b5* or a heme-based cis-trans carotene isomerase Z-ISO (Beltrán et al., 2015). In accordance, DGK4 mutations, which affect the heme binding site, should produce a reduced heme absorption spectrum, as demonstrated for Z-ISO (Beltrán et al., 2015). Indeed, H350L and Y379L *dgk4* mutants showed reduced Soret band intensities of about 50% and 70%, respectively (Fig. 2D). As the Soret bands were still present in the mutants, albeit attenuated, we can expect a similar behavior in their reductions and NO spectra, which we did observe with the H350L mutant protein (Fig. S4). Overall, the H350L *dgk4* mutant recorded a much larger decrease in reduced Soret bands than observed with DGK4 WT at low NO donor concentration (0.25 mM DEA NONOate) and also required a slightly longer time (∼5 min more than DGK4 WT) to recover its oxidized Soret peak (410 nm) when exposed to air (Fig. S4). Together with a marked reduction in Soret band intensities of *dgk4* mutants, these results can be interpreted as a weakening of the heme environment. Our data are consistent with a recently identified *Arabidopsis* protein, AtLRB3 (At4g01160), which, like DGK4, harbors a H-NOX-like center that yields canonical spectroscopic behavior of H-NOX proteins, and for which mutation of the heme iron-coordinating histidine impairs the NO response (Zarban et al., 2019).

Based on protein sequence analysis we previously predicted DGK4 to be a bifunctional catalytic protein with a canonical kinase domain capable of converting *sn*-1,2-diacylglycerol (DAG) with ATP into the corresponding phosphatidic acid (PA), but, importantly, with a hypothetical guanylyl cyclase (GC) center capable of catalyzing the formation of cGMP from GTP (Wong et al., 2013; Domingos et al., 2015; Xu et al., 2018; Su et al., 2019). Our prediction was recently confirmed by others (Vaz Dias et al., 2019). Thus, we next focused on the catalytic activity of DGK4. Both cGMP and, more strongly, NO inhibited DGK4 kinase activity but NO did not affect the GC activity (Fig. 2E). Mutations in the H-NOX center did not affect the kinase activity of DGK4, as both H350L and Y379L *dgk4* mutants were functional and inhibited by NO to a similar degree as the WT (Fig. S5). Although this result could nullify the hypothesis that the H-NOX center of *dgk4-1* works as a NO sensor, it must be considered that, although there is a reduction of intensity and slower recovery upon oxidation, there are still changes in the Soret band in the mutants, thus revealing some NO binding. Given that both the enzyme and the NO steady concentrations *in vivo* should be much lower (Prado et al., 2004), the range of physiological sensitization to NO might therefore not be captured given the conditions of the enzymatic assays.

Another conceivable possibility that we cannot overrule at this point is that NO-induced S-nitrosylation is also taking place, as reported for other kinases (Hu et al., 2017; Liu et al., 2017). DGK4 displays five S-nitrosylation sites on C62, C138, C174, C260 and C334 (SNOSite, csb.cse.yzu.edu.tw/SNOSite/Prediction.html; Lee et al., 2011). Of these, C138 and C174 are in the kinase/GC domains but no S-nitrosylation sites have been predicted at the H-NOX center. Either way, as DGK4 is localized in the cytosolic region of the PT apex (Vaz Dias et al., 2019), our results are consistent with a signaling role for DGK4 in transducing NO-binding into lipid-, cGMP- or Ca^{2+}-dependent downstream responses. This conclusion is based on the fact that DGKs are known to convert DAG to PA, which in turn is essential for PT growth (Pleskot et al., 2012; Potocký et al., 2014) and the mobilization of Ca^{2+} (Monteiro et al., 2005; Prado et al., 2008). Our biochemical data also show that, although the kinase activity of DGK4 is inhibited by cGMP, the GC activity of DGK4 is unaffected by NO, thus implying that the reduced NO response of *dgk4-1* PTs might be achieved primarily through the PA-dependent lipid/Ca^{2+} signaling pathways rather than the activation of its GC moonlighting center. Although the existence of a cyclic nucleotide signaling paradigm in plants is controversial (Gehring and Turek, 2017; Świeżawska et al., 2018), cGMP has been shown to activate Ca^{2+} currents by the cyclic nucleotide-gated channel 18 (CNGC18) localized at the tip of PTs (Gao et al., 2016).

In summary, Fig. 2F depicts a hypothetical mechanism for NO action in PTs. In this model, NO could have two distinct targets in

Development (2020) 147, dev183715. doi:10.1242/dev.183715

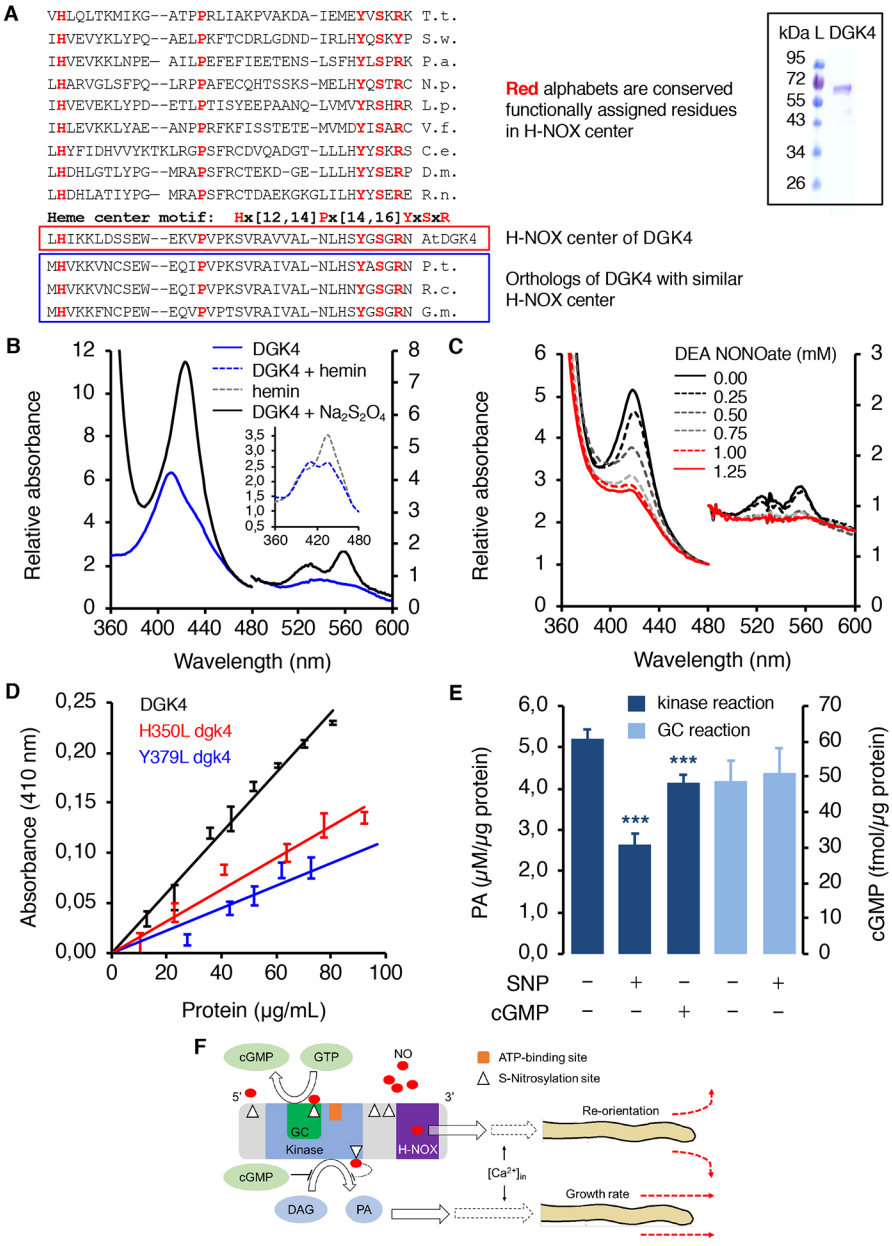

Fig. 2. DGK4 has NO-responsive spectral and catalytic activity. (A) The region H350 to R383 in DGK4 contains amino acid residues of annotated heme centers of gas-responsive proteins, as shown in the alignment of *Thermoanaurobacter tengcongensis* (T.t.; GI: 3566245696), *Shewanella woodyi* (S.w.; GI: 169812443), *Pseudoalteromonas atlantica* (P.a.; GI: 109700134), *Nostoc punctiforme* (N.p.; GI: 126031328), *Legionella pneumophila* (L.p.; GI: 52841290), *Vibrio fischeri* (V.f.; GI: 59713254), *Caenorhabditis elegans* (C.e.; GI: 52782806), *Drosophila melanogaster* (D.m.; GI: 861203), *Rattus norvegicus* (R.n.; GI:27127318), *Arabidopsis thaliana* (AtDGK4; GI: 145359366), *Populus trichocarpa* (P.t.; GI: 224143809), *Ricinus communis* (R.c.; GI: 255581896) and *Glycine max* (G.m.; GI: 356567686) hemoproteins. Inset: recombinant DGK4 was generated and purified according to procedures described in the Materials and Methods. (B) DGK4 (inset) contains a cytochrome b_5 type heme center, as indicated by the electronic absorption spectra in the ferric and ferrous states (Table S1). (C) UV-visible light characterization of recombinant DGK4 reveals that NO attenuates the Soret peak of the ferrous heme center in a concentration-dependent manner. (D) The H350L and Y379L *dgk4* mutants have reduced heme binding. At 80 µg of protein, H350L and Y379L dgk4 have Soret peaks that are 0.5- and 0.3-fold of DGK4 (*n*=3; *n*=independent experiments). (E) The kinase activity of DGK4 was reduced in the presence of SNP (1 mM) or cGMP (1 mM) but the GC activity was unaffected by SNP (1 mM) (*n*=3; *n*=independent experiments). ***P<0.0005 compared with the activity of DGK4 with no SNP or cGMP. (F) A model of DGK4 signaling roles in mediating NO-dependent PT growth and re-orientation responses. NO modulates PT re-orientation responses by binding to the H-NOX center and/or inhibiting the kinase activity, possibly via S-nitrosylation at C138 and/or C174, yielding reduced PA, which in turn modulates cytosolic Ca^{2+}. Differential kinetics of these mechanisms, different affinities of NO binding and the role of cGMP inhibiting the kinase activity but unaffected by NO could generate the sequential effects on PT retardation, re-orientation and growth resumption responses.

DGK4: on the one hand, NO modulates PT re-orientation responses by binding to the H-NOX center of DGK4, leading to a PA reduction; on the other hand, NO inhibits the kinase and GC activities of DGK4 via S-nitrosylation at C138 and/or C174. We hypothesize that differential kinetics of these mechanisms (H-NOX is predicted to occur much faster), different affinities of NO binding (defining different intervals of NO perception), and the role of cGMP (which we found to inhibit the kinase activity but is not affected by NO) could generate the sequential effects observed during our slowing/re-orientation assays, and the lack of thereof in the mutant. The readout of DGK-4-mediated reactions would be transduced into variations of PA, which is known to interplay with Ca^{2+} signaling, possibly triggering other downstream paths resulting in vesicular trafficking and/or alterations in actin dynamics (Li et al., 1999; Chen et al., 2003). In agreement with this interpretation, *dgk4* PTs have recently been reported to exhibit altered mechanical properties with downregulation of a cyclase-associated protein CAP1, which is involved in actin dynamics, and a general downregulation of phosphoinositide metabolism (Vaz Dias et al., 2019).

Importantly, the slowing down of PTs is necessary for optimizing the perception of chemical cues (Stewman et al., 2010); this constitutes a plausible explanation for the loss of chemotropic response in the mutant and contributes to the observed seed-set reduction. As a fast-diffusible gas, NO is well suited to perform fine-tuning of rapid cell-cell communications, such as the pollen-stigma interactions (Prado et al., 2008; Feijó, 2010; Domingos et al., 2015), and we posit that DGK4 might be an important sensing input mechanism of NO to regulate plant reproduction.

MATERIALS AND METHODS

Plant materials and growth conditions

Two mutant *Arabidopsis* lines (SALK_151239 and SALK_145081) with T-DNA insertions at the promoter of *DGK4* were obtained from the Nottingham Arabidopsis Stock Center and progenies were PCR screened for homozygosity of mutant (T-DNA+*DGK4* reverse primer) and WT (*DGK4*

Development (2020) 147, dev183715. doi:10.1242/dev.183715

promoter forward+*DGK4* reverse primer) chromosomes (Table S2). The homozygous mutant alleles were subsequently referred to as *dgk4-1* and *dgk4-2*, respectively. The T-DNA insertion sites were confirmed by sequencing (KAUST Bioscience Core Lab). All seeds were stratified at 4°C for 3 days. Col-0 (wild-type) and mutant lines were grown on soil (Jiffy) containing 50% (w/v) of vermiculite in Percival growth chambers (CLF Plant Climatics) at 22±2°C and 60% of relative humidity under long day (16 h light) photoperiod (100 µM photons m^{-2} s^{-1}).

Characterization of *dgk4* mutant plants

RNA was extracted from the pollen of ∼300 flowers of WT and *dgk4-1* mutants (Qiagen) and cDNA synthesized using SuperScript III reverse transcriptase according to manufacturer's protocols (Invitrogen). The cDNA was subjected to semi-quantitative RT-PCR with *DGK4* gene-specific primers (Table S2) on an AB thermal cycler (Bio-Rad); *DGK4* gene expression was normalized against that of protein phosphatase 2A subunit A3, *PP2AA3* (At1g13320) (Table S2), using the ImageLab software (Bio-Rad).

In vitro pollen germination

In vitro pollen germination was performed as previously described (Prado et al., 2004, 2008) but with optimized germination medium for *Arabidopsis* (Boavida and McCormick, 2007) with or without the NO sources sodium nitroprusside (SNP) or DEA NONOate. The growth of at least 100 PTs was measured on a Nikon Eclipse TE2000-S inverted microscope equipped with an Andor iXon3 camera across a range of pH values (pH 6.5-8.5) and in optimal (5 mM) and low (100 µM) Ca^{2+} media. In NO-treated pollen germination and PT growth experiments, at least 150 unique pollen or PTs were considered. Image frames covering the entire growth area of the culture dish that is mounted on automated stage were acquired using the Nikon Eclipse TE2000-S inverted microscope, which is equipped with a Hamamatsu Flash28s CMOS camera. The PT lengths were measured using NeuronJ (Meijering et al., 2004). For PT re-orientation studies, PTs were challenged with a NO artificial point source by loading with glass micropipettes (OD 1.5 mm, ID 1.2 mm, WPI) pulled to a tip with a ∼5 µm aperture filled with 10 mM SNAP (s-nitroso-acethilpenilcilamine) on agarified (1%) germination medium. Typically, the pipette tip was placed 60 µm away from the growing PT tip using a nanometer-stepper, motor-driven, three-dimensional positioner (Science Wares). Growth and bending responses of growing PTs were monitored by imaging using a Nikon Eclipse TE2000-S inverted microscope (PlanApo 40×, NA 1.3) equipped with an Andor iXon3 camera and the bending angles measured using ImageJ (Schneider et al., 2012).

PT growth *in planta*

PT growth in the pistil of hand-pollinated WT and *dgk4-1* plants was examined by collecting the pistils at different time points (3-8 h) after pollination. Aniline blue staining of PTs in the pistil was performed as described previously (Mori et al., 2006) and PT length in the pistil was measured using ImageJ (Schneider et al., 2012).

Reproductive fitness test

The reproductive fitness of *dgk4-1* was examined by crossing emasculated WT (ecotype Col-0) flowers with pollen from both WT and *dgk4-1*. In detail, a ∼50:50 mixture of pollen from Col-0 (rr) and *dgk4-1* (RR) was brushed onto an emasculated Col-0 flower, where pollen was effectively Rr crossed onto the Col-0 female (rr). If there was no bias in fitness, then there should be a 50% kanamycin-resistant and 50% kanamycin-susceptible phenotype. If the Col-0 pollen is fitter, then fewer than half of the offspring will be kanamycin resistant. The desiccated seeds were collected, surface sterilized and stored at 4°C for 3 days and then grown on Murashige and Skoog agar medium (1.1% w/v) containing 100 µg/ml kanamycin (Sigma-Aldrich). The proportion of WT to *dgk4-1* seeds were scored after 7 days of growth (n>70).

Protein expression and purification

A Gateway-compatible clone (DKLAT5G57690.1) containing the full-length coding sequence of *DGK4* was purchased from Arabidopsis Biological Resource Center. The DGK4 sequence was recombined into the pDEST17 his-tagged expression vector and transformed into *E. coli* BL21 A1 (Invitrogen). Expression of recombinant DGK4 was induced with 0.2% (w/v) L-arabinose. Cells were lysed in a guanidium lysis buffer and the supernatant loaded onto a Ni-NTA agarose column for affinity purification under denaturing conditions using urea-containing buffers. Denatured recombinant DGK4 was refolded by gradual dilution of urea in a linear gradient using an AKTA fast protein liquid chromatography (GE Healthcare). Hemin (30 µg/ml) was added to the refolding buffers to allow for the incorporation of heme into DGK4 as it assumes native conformation. Excess hemin was removed by size exclusion and recombinant DGK4 stored in 'buffer' containing 20 mM $Na_2H_2PO_4$, 500 mM NaCl, 500 mM sucrose, 100 mM non-detergent sulfobetaines (NDSB), 0.05% (w/v) polyethylene glycol (PEG), 4 mM reduced glutathione, 0.04 mM oxidized glutathione and SIGMAFAST protease inhibitor cocktail (1 tablet per 100 ml solution).

Two single *dgk4* mutants (H350L and Y379L) were constructed using site directed mutagenesis by PCR (Ho et al., 1989). To construct the H350L *dgk4* mutant, two overlapping fragments of the DGK4 coding sequence both incorporating the mutation, were amplified from the pDEST17-*DGK4* plasmid using the respective *DGK4* F and *DGK4* H-L R (first fragment amplification), and *DGK4* H-L F and *DGK4* R (second fragment amplification) primer pairs (Table S2). The two overlapping fragments both incorporating the mutations were then used as templates for a PCR reaction using the full-length *DGK4* F and *DGK4* R primer pairs (Table S2), which generated a full-length *dgk4* H350L mutant sequence. The *dgk4* Y379L mutant was generated using the same method but with the following mutagenic primers pairs, *DGK4* F and *DGK4* Y-L R, and *DGK4* Y-L F and *DGK4* R (Table S2). The *DGK4* mutant PCR products were inserted into the PCR8/GW/TOPO vector (Invitrogen) by TA cloning, recombined into the pDEST17 his-tagged expression vector and transformed into *E. coli* BL21 A1 (Invitrogen). Mutant *dgk4* was expressed and affinity purified in the same manner as DGK4.

UV-visible absorption spectroscopy

The UV-visible spectra of affinity purified recombinant DGK4 (200 µg/ml) was recorded on a PHERAstar FS micro-plate reader (BMG Labtech). The heme environment of DGK4 was characterized by the addition of a reducing agent, sodium dithionite ($Na_2S_2O_4$), to a final concentration of 10 mM and absorbance was immediately measured and examined for spectral changes. The protein sample was then exposed to air and any recovery of the oxidized peak was monitored by the same spectra measurements at 5 min intervals. The heme-NO complex was generated by immediately adding the NO donor DEA NONOate to a pre-reduced recombinant DGK4 before making the same spectral measurements.

DAG kinase and GC assays

DAG kinase assay and phospholipid extraction was performed using 30 µg purified recombinant protein in a reaction mixture containing 40 mM Bis-Tris (pH 7.5), 5 mM $MgCl_2$, 0.1 mM EDTA, 1 mM spermine, 0.5 mM dithiothreitol, 1 mM sodium deoxycholate, 0.02% (v/v) Triton X-100, 500 µM 1,2-DOG and 1 mM ATP in the absence or presence of 1 mM SNP or 0.65 mM DEA NONOate. PA generated from the reactions was measured using the Total Phosphatidic Acid Assay Kit (Cayman Chemical) according to the manufacturer's protocol.

A GC assay was performed using 10 µg purified recombinant protein in a reaction mixture containing 50 mM Tris-HCl (pH 7.5), 1 mM GTP, 5 mM $MgCl_2$ or $MnCl_2$, in the absence or presence of 1 mM SNP or 0.65 mM DEA NONOate. cGMP generated from the reactions was measured using the cGMP enzyme immunoassay (EIA) Biotrak System according to the manufacturer's acetylation protocol (GE Healthcare).

Chemicals and statistical analysis

All chemicals were purchased from Sigma-Aldrich unless stated otherwise. Statistical analyses were performed using an unpaired, one-tailed Student's t-test. Significance was set to a threshold of P<0.05 and n values represent the number of biological replicates.

Competing interests

The authors declare no competing or financial interests.

Author contributions

Conceptualization: A.W., J.A.F., C.G.; Methodology: M.P., J.A.F., C.G.; Validation: M.P., J.A.F.; Formal analysis: A.W., M.P., J.A.F., C.G.; Investigation: A.W., L.D., M.P., J.A.F., C.G.; Data curation: A.W., M.P., J.E., J.A.F., C.G.; Writing - original draft: A.W.; Writing - review & editing: L.D., M.P., J.E., J.A.F., C.G.; Visualization: J.A.F.; Supervision: J.A.F., C.G.; Project administration: J.A.F., C.G.; Funding acquisition: J.A.F., C.G.

Funding

This research was supported by the King Abdullah University of Science and Technology (to C.G.); the National Science Foundation (MCB-1616437 and MCB-1930165 to J.A.F.); the National Natural Science Foundation of China (31850410470 to A.W.); and the Zhejiang Provincial Natural Science Foundation of China (LQ19C130001 to A.W.).

Supplementary information

Supplementary information available online at
http://dev.biologists.org/lookup/doi/10.1242/dev.183715.supplemental

Peer review history

The peer review history is available online at
https://dev.biologists.org/lookup/doi/10.1242/dev.183715.reviewer-comments.pdf

References

Aller, I., Rouhier, N. and Meyer, A. J. (2013). Development of roGFP2-derived redox probes for measurement of the glutathione redox potential in the cytosol of severely glutathione-deficient rml1 seedlings. *Front. Plant Sci.* **4**, 506. doi:10.3389/fpls.2013.00506

Astier, J., Mounier, A., Santolini, J., Jeandroz, S. and Wendehenne, D. (2019). The evolution of nitric oxide signalling diverges between the animal and the green lineages. *J. Exp. Bot.* **70**, 4355-4364. doi:10.1093/jxb/erz088

Beltrán, J., Kloss, B., Hosler, J. P., Geng, J., Liu, A., Modi, A., Dawson, J. H., Sono, M., Shumskaya, M., Ampomah-Dwamena, C. et al. (2015). Control of carotenoid biosynthesis through a heme-based cis-trans isomerase. *Nat. Chem. Biol.* **11**, 598-605. doi:10.1038/nchembio.1840

Boavida, L. C. and McCormick, S. (2007). Temperature as a determinant factor for increased and reproducible in vitro pollen germination in Arabidopsis thaliana. *Plant J.* **52**, 570-582. doi:10.1111/j.1365-313X.2007.03248.x

Chen, C. Y.-H., Cheung, A. Y. and Wu, H.-M. (2003). Actin-depolymerizing factor mediates Rac/Rop GTPase-regulated pollen tube growth. *Plant Cell* **15**, 237-249. doi:10.1105/tpc.007153

Dai, Z., Farquhar, E. R., Arora, D. P. and Boon, E. M. (2012). Is histidine dissociation a critical component of the NO/H-NOX signaling mechanism? Insights from X-ray absorption spectroscopy. *Dalton Trans.* **41**, 7984-7993. doi:10.1039/c2dt30147d

Domingos, P., Prado, A. M., Wong, A., Gehring, C. and Feijo, J. A. (2015). Nitric oxide: a multitasked signaling gas in plants. *Mol. Plant* **8**, 506-520. doi:10.1016/j.molp.2014.12.010

Feijó, J. A. (2010). The mathematics of sexual attraction. *J. Biol.* **9**, 18. doi:10.1186/jbiol233

Gao, Q.-F., Gu, L.-L., Wang, H.-Q., Fei, C.-F., Fang, X., Hussain, J., Sun, S.-J., Dong, J.-Y., Liu, H. and Wang, Y.-F. (2016). Cyclic nucleotide-gated channel 18 is an essential Ca^{2+} channel in pollen tube tips for pollen tube guidance to ovules in Arabidopsis. *Proc. Natl. Acad. Sci. USA* **113**, 3096-3101. doi:10.1073/pnas.1524629113

Gehring, C. and Turek, I. S. (2017). Cyclic nucleotide monophosphates and their cyclases in plant signaling. *Front. Plant Sci.* **8**, 1704. doi:10.3389/fpls.2017.01704

He, J.-M., Bai, X.-L., Wang, R.-B., Cao, B. and She, X.-P. (2007). The involvement of nitric oxide in ultraviolet-B-inhibited pollen germination and tube growth of Paulownia tomentosa in vitro. *Physiol. Plant.* **131**, 273-282. doi:10.1111/j.1399-3054.2007.00955.x

Ho, S. N., Hunt, H. D., Horton, R. M., Pullen, J. K. and Pease, L. R. (1989). Site-directed mutagenesis by overlap extension using the polymerase chain reaction. *Gene* **77**, 51-59. doi:10.1016/0378-1119(89)90358-2

Hu, J., Yang, H., Mu, J., Lu, T., Peng, J., Deng, X., Kong, Z., Bao, S., Cao, X. and Zuo, J. (2017). Nitric oxide regulates protein methylation during stress responses in plants. *Mol. Cell* **67**, 702-710.e4. doi:10.1016/j.molcel.2017.06.031

Lamattina, L., García-Mata, C., Graziano, M. and Pagnussat, G. (2003). Nitric oxide: the versatility of an extensive signal molecule. *Annu. Rev. Plant Biol.* **54**, 109-136. doi:10.1146/annurev.arplant.54.031902.134752

Lee, T.-Y., Chen, Y.-J., Lu, T.-C., Huang, H.-D. and Chen, Y.-J. (2011). SNOSite: exploiting maximal dependence decomposition to identify cysteine S-nitrosylation with substrate site specificity. *PLoS ONE* **6**, e21849. doi:10.1371/journal.pone.0021849

León, J. and Costa-Broseta, A. (2019). Present knowledge and controversies, deficiencies and misconceptions on nitric oxide synthesis, sensing, and signaling in plants. *Plant Cell Environ.* **43**, 1-15. doi:10.1111/pce.13617

Li, H., Lin, Y., Heath, R. M., Zhu, M. X. and Yang, Z. (1999). Control of pollen tube tip growth by a Rop GTPase-dependent pathway that leads to tip-localized calcium influx. *Plant Cell* **11**, 1731-1142. doi:10.2307/3871050

Liu, J.-Z., Duan, J., Ni, M., Liu, Z., Qiu, W.-L., Whitham, S. A. and Qian, W.-J. (2017). S-Nitrosylation inhibits the kinase activity of tomato phosphoinositide-dependent kinase 1 (PDK1). *J. Biol. Chem.* **292**, 19743-19751. doi:10.1074/jbc.M117.803882

McInnis, S. M., Desikan, R., Hancock, J. T. and Hiscock, S. J. (2006). Production of reactive oxygen species and reactive nitrogen species by angiosperm stigmas and pollen: potential signalling crosstalk? *New Phytol.* **172**, 221-228. doi:10.1111/j.1469-8137.2006.01875.x

Meijering, E., Jacob, M., Sarria, J. C.-F., Steiner, P., Hirling, H. and Unser, M. (2004). Design and validation of a tool for neurite tracing and analysis in fluorescence microscopy images. *Cytometry A* **58**, 167-176. doi:10.1002/cyto.a.20022

Miraglia, E., De Angelis, F., Gazzano, E., Hassanpour, H., Bertagna, A., Aldieri, E., Revelli, A. and Ghigo, D. (2011). Nitric oxide stimulates human sperm motility via activation of the cyclic GMP/protein kinase G signaling pathway. *Reproduction* **141**, 47-54. doi:10.1530/REP-10-0151

Monteiro, D., Liu, Q., Lisboa, S., Scherer, G. E. F., Quader, H. and Malhó, R. (2005). Phosphoinositides and phosphatidic acid regulate pollen tube growth and reorientation through modulation of $[Ca^{2+}]$c and membrane secretion. *J. Exp. Bot.* **56**, 1665-1674. doi:10.1093/jxb/eri163

Mori, T., Kuroiwa, H., Higashiyama, T. and Kuroiwa, T. (2006). Generative cell specific 1 is essential for angiosperm fertilization. *Nat. Cell Biol.* **8**, 64-71. doi:10.1038/ncb1345

Pleskot, R., Pejchar, P., Bezvoda, R., Lichtscheidl, I. K., Wolters-Arts, M., Marc, J., Žárský, V. and Potocký, M. (2012). Turnover of phosphatidic acid through distinct signaling pathways affects multiple aspects of pollen tube growth in tobacco. *Front. Plant Sci.* **3**, 54. doi:10.3389/fpls.2012.00054

Potocký, M., Pleskot, R., Pejchar, P., Vitale, N., Kost, B. and Žárský, V. (2014). Live-cell imaging of phosphatidic acid dynamics in pollen tubes visualized by Spo20p-derived biosensor. *New Phytol.* **203**, 483-494. doi:10.1111/nph.12814

Prado, A. M., Porterfield, D. M. and Feijó, J. A. (2004). Nitric oxide is involved in growth regulation and re-orientation of pollen tubes. *Development* **131**, 2707-2714. doi:10.1242/dev.01153

Prado, A. M., Colaço, R., Moreno, N., Silva, A. C. and Feijó, J. A. (2008). Targeting of pollen tubes to ovules is dependent on nitric oxide (NO) signaling. *Mol. Plant* **1**, 703-714. doi:10.1093/mp/ssn034

Russwurm, M. and Koesling, D. (2004). NO activation of guanylyl cyclase. *EMBO J.* **23**, 4443-4450. doi:10.1038/sj.emboj.7600422

Schneider, C. A., Rasband, W. S. and Eliceiri, K. W. (2012). NIH Image to ImageJ: 25 years of image analysis. *Nat. Meth.* **9**, 671-675. doi:10.1038/nmeth.2089

Sengoku, K., Tamate, K., Yoshida, T., Takaoka, Y., Miyamoto, T. and Ishikawa, M. (1998). Effects of low concentrations of nitric oxide on the zona pellucida binding ability of human spermatozoa. *Fertil. Steril.* **69**, 522-527. doi:10.1016/S0015-0282(97)00537-2

Stewman, S. F., Jones-Rhoades, M., Bhimalapuram, P., Tchernookov, M., Preuss, D. and Dinner, A. R. (2010). Mechanistic insights from a quantitative analysis of pollen tube guidance. *BMC Plant Biol.* **10**, 32. doi:10.1186/1471-2229-10-32

Su, B., Qian, Z., Li, T., Zhou, Y. and Wong, A. (2019). PlantMP: a database for moonlighting plant proteins. *Database* **2019**, baz050. doi:10.1093/database/baz050

Świeżawska, B., Duszyn, M., Jaworski, K. and Szmidt-Jaworska, A. (2018). Downstream targets of cyclic nucleotides in plants. *Front. Plant Sci.* **9**, 1428. doi:10.3389/fpls.2018.01428

Vaz Dias, F., Serrazina, S., Vitorino, M., Marchese, D., Heilmann, I., Godinho, M., Rodrigues, M. and Malhó, R. (2019). A role for diacylglycerol kinase 4 in signalling crosstalk during Arabidopsis pollen tube growth. *New Phytol.* **222**, 1434-1446. doi:10.1111/nph.15674

Walker, F. A., Ribeiro, J. M. and Montfort, W. R. (1999). Novel nitric oxide-liberating heme proteins from the saliva of bloodsucking insects. *Met. Ions Biol. Syst.* **36**, 621-663. doi:10.1201/9780203747605-19

Wang, Y., Chen, T., Zhang, C., Hao, H., Liu, P., Zheng, M., Baluška, F., Šamaj, J. and Lin, J. (2009). Nitric oxide modulates the influx of extracellular Ca^{2+} and actin filament organization during cell wall construction in Pinus bungeana pollen tubes. *New Phytol.* **182**, 851-862. doi:10.1111/j.1469-8137.2009.02820.x

Wang, Y.-H., Li, X.-C., Zhu-Ge, Q., Jiang, X., Wang, W.-D., Fang, W.-P., Chen, X. and Li, X.-H. (2012). Nitric oxide participates in cold-inhibited Camellia sinensis pollen germination and tube growth partly via cGMP in vitro. *PLoS ONE* **7**, e52436. doi:10.1371/journal.pone.0052436

Wendehenne, D., Pugin, A., Klessig, D. F. and Durner, J. (2001). Nitric oxide: comparative synthesis and signaling in animal and plant cells. *Trends Plant Sci.* **6**, 177-183. doi:10.1016/S1360-1385(01)01893-3

Wong, A., Donaldson, L. and Gehring, C. (2013). The enzymatic activity of Arabidopsis diacylglycerol kinase 4 (ATDGK4) is regulated by nitric oxide. 16th International Workshop on Plant Membrane Biology. https://f1000research.com/posters/1093019.

Wong, A., Tian, X., Gehring, C. and Marondedze, C. (2018). Discovery of novel functional centers with rationally designed amino acid motifs. *Comput. Struct. Biotechnol. J.* **16**, 70-76. doi:10.1016/j.csbj.2018.02.007

Xu, N., Fu, D., Li, S., Wang, Y. and Wong, A. (2018). GCPred: a web tool for guanylyl cyclase functional center prediction from amino acid sequence. *Bioinformatics* **34**, 2134-2135. doi:10.1093/bioinformatics/bty067

Zarban, R., Vogler, M., Wong, A., Eppinger, J., Al-Babili, S. and Gehring, C. (2019). Discovery of a nitric oxide-responsive protein in Arabidopsis thaliana. *Molecules* **24**, E2691. doi:10.3390/molecules24152691

Figure S1. Characterization of *dgk4* T-DNA insertion mutant plants

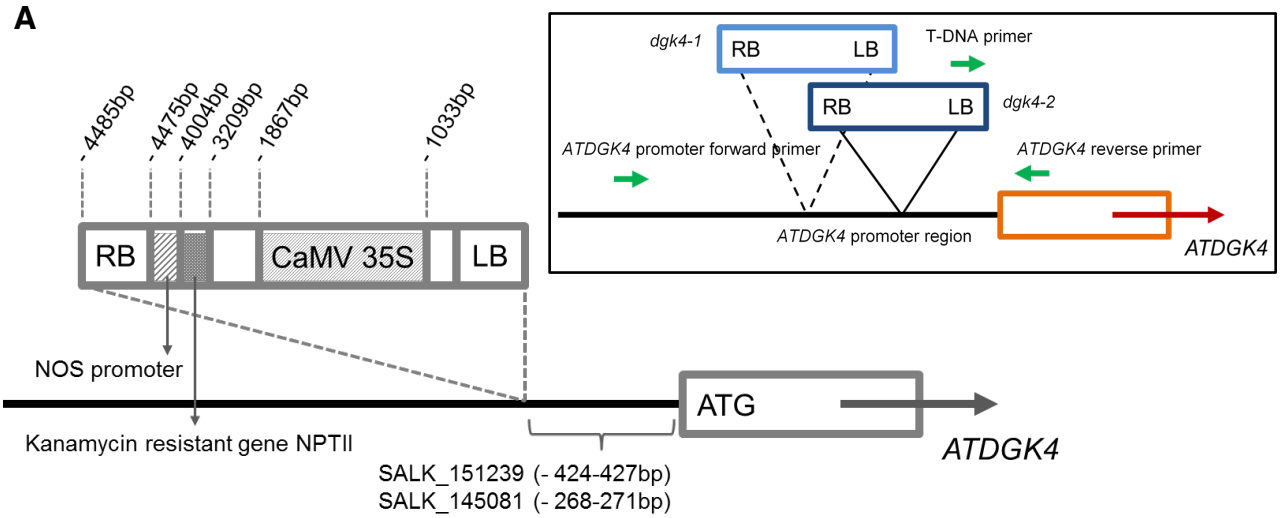

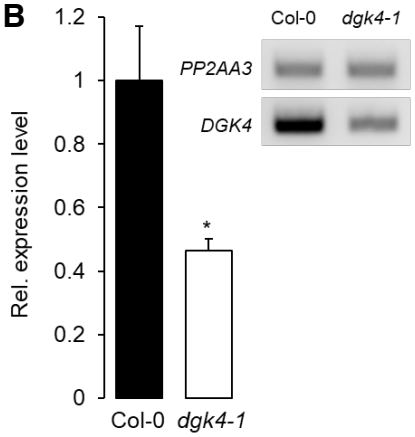

Legend:

SALK_151239 is designated as *dgk4-1*

SALK_145081 is designated as *dgk4-2*

(**A**) Schematic view of T-DNA insertion sites of *dgk4* mutants. Location and content of SALK T-DNA insertions are labelled. LB and RB indicate Left Border and Right Border of the T-DNA respectively. Inset: Green arrows indicate the position and direction of primers (see Table S2) used in RT-PCR to determine *DGK4* expression levels. (**B**) *dgk4-1* pollen has reduced *DGK4* mRNA levels as estimated by semi-quantitative RT-PCR. ** = P < 0.05* compared to *DGK4* mRNA levels of *Col-0* pollen and gel pictures are representative of three independently derived biological replicates.

Figure S2. Homozygous *dgk4-2* PT has slower growth rate and reduced NO-dependent growth response

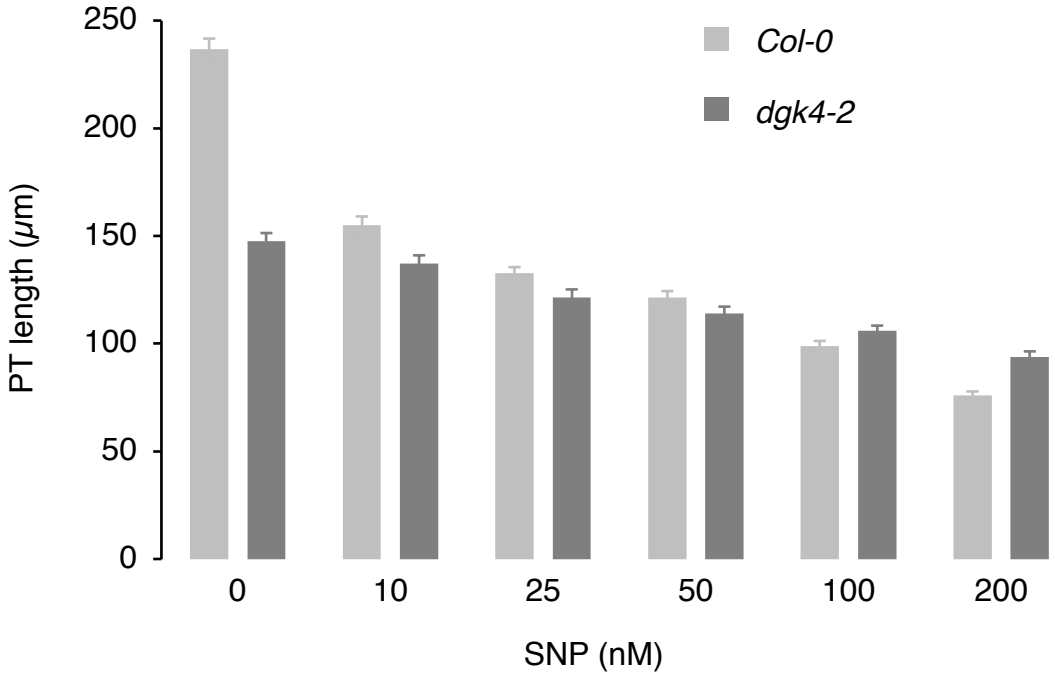

NO-dependent inhibition of *dgk4-2* PT growth is reduced compared to that of *Col-0*. NO was provided by either SNP. *In vitro* pollen germination was performed as detailed previously (Prado et al., 2004; Prado et al., 2008) and PT length was analyzed by capturing images covering the entire growth area of the culture dish that is mounted on an automated stage using the Nikon Eclipse TE2000-S inverted microscope equipped with a Hamamatsu Flash28s CMOS camera. The PT lengths were then measured using NeuronJ (Meijering et al., 2004). Error bars represent s.e.m. ($n > 150$).

Figure S3. Variability of PT growth responses to NO-generating pipette sources

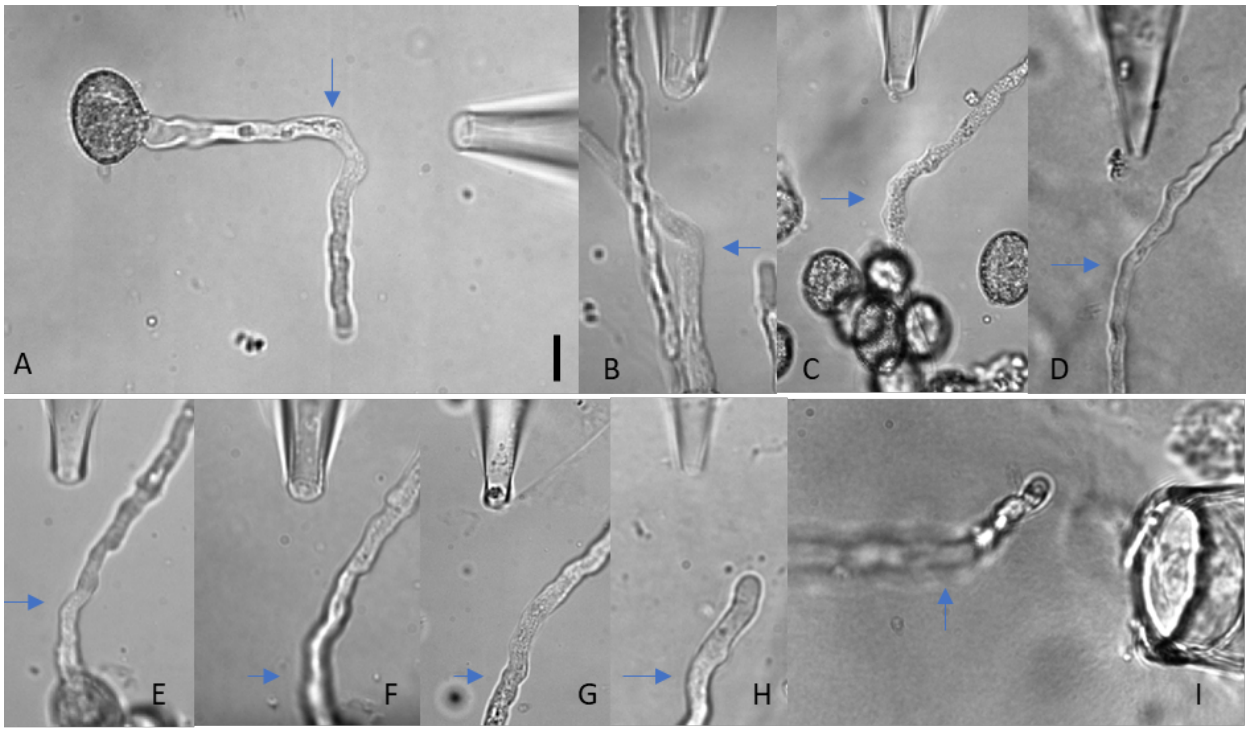

Top row: WT, bottom row: *dgk4-1.* Blue arrows represent the time point of the tip when the sources were positioned. Individual *Col-0* and *dgk4-1* PT bending angles were 37°, 35°, 28°, 28°, 90°, 48°, 29°, 69°, 44° and 50°, and 15°, 9°, 21°, 14°, 33°, 21°, 31°, 32°, 26° and 27° respectively. While a lone 90º orientation was observed for WT (**A**), most tubes show angles around 35-40º (**B**, **C** and **D**). They all showed clear, elbow-like, point of inflections when approaching the critical NO concentration to produce a response (see also Figure 1D, *Col-0*). This elbow turns were also observed in lily (Prado et al., 2004) and correspond to a slowdown/halt of the growth rate, followed by turning of the PT (see movie S1). In contrast, *dgk4-1* PTs always show smoother or softer turns around 20º (**E**, **F**, **G** and **H**), with variable impacts on the growth rate, from full-stop to apparent no effect. On trying to push the boundary of how much *dgk4-1* PTs can turn, we made experiments with pipettes more than twice the tip diameter and with ca. twice the concentration of SNP. Even under these extreme conditions (**I**) the observed turning angle was below the average angle observed for WT and with no elbow-like turn. Bar represents 10 μm.

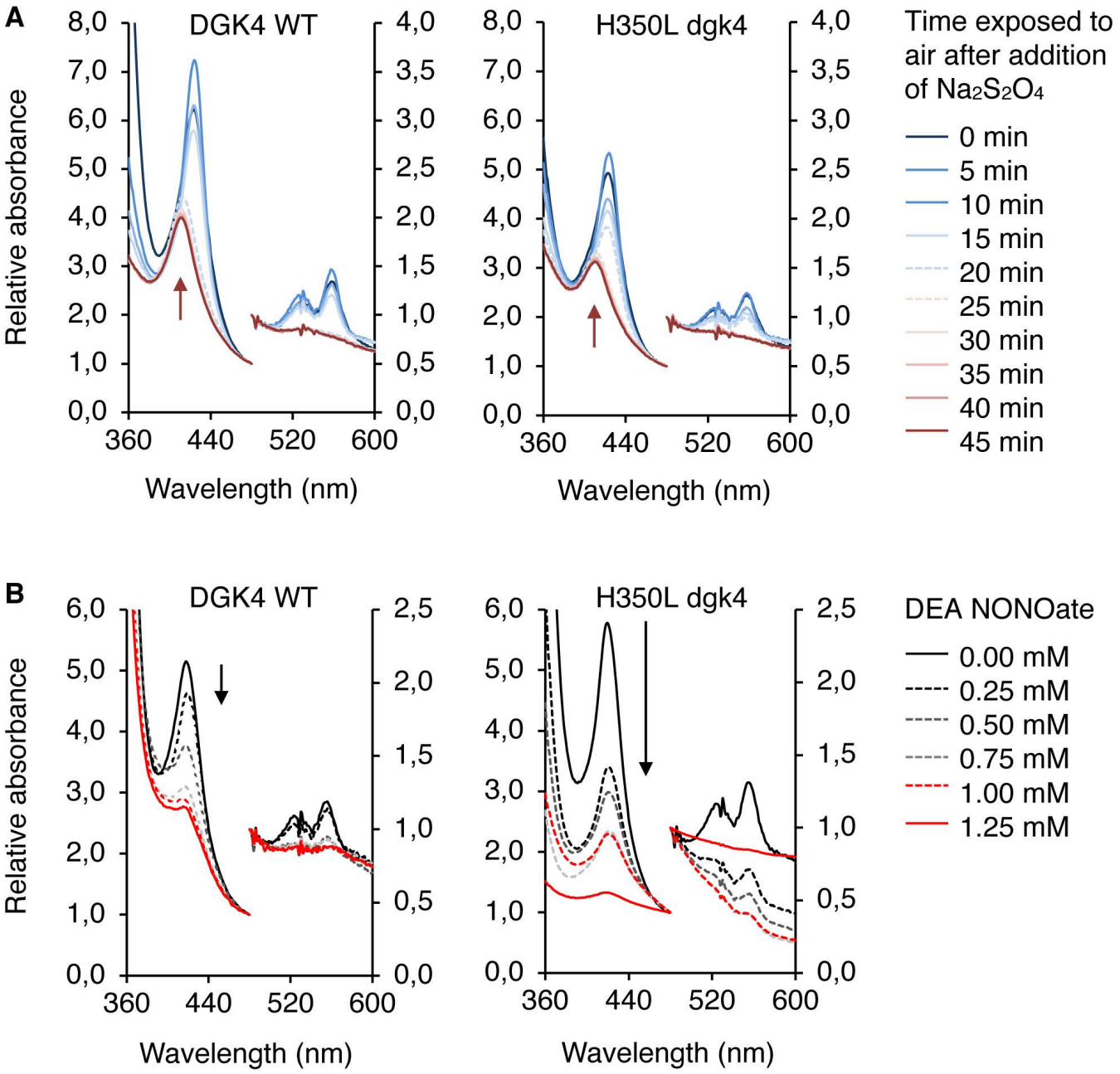

Figure S4. DGK4 harboring point mutation at the H-NOX-like center yields spectral behavior similar to WT

(**A**) UV-vis characterization reveals that the Soret peaks (410 nm) of 80 μg DGK4 WT and H350L dgk4 mutant proteins were both red-shifted to 424 nm accompanied by the emergence of distinct α (558 nm) and β (526 nm) bands when reduced with sodium

dithionite. The oxidized Soret peaks (410 nm) (red arrows) of both DGK4 WT and H350L dgk4 mutant were fully recovered after 20 and 25 min of exposure to air respectively. (**B**) Addition of DEA NONOate to reduced DGK4 and H350L dgk4 attenuates the Soret absorption (424 nm) in a concentration dependent manner where the Soret, *β*- and *α*-peaks vanish with increasing concentration of the NO donor. H350L dgk4 mutant recorded a much larger decrease in reduced Soret bands than that observed with DGK4 WT at low NO donor concentration (0.25 mM DEA NONOate) (black arrows) while also requiring a slightly longer time (~ 5 min more than DGK4 WT) (red arrows) to recover its oxidized Soret peak (410 nm) when exposed to air.

Figure S5. Kinase activities of DGK4 and mutant dgk4 harboring point mutations at the H-NOX-like center were inhibited by NO

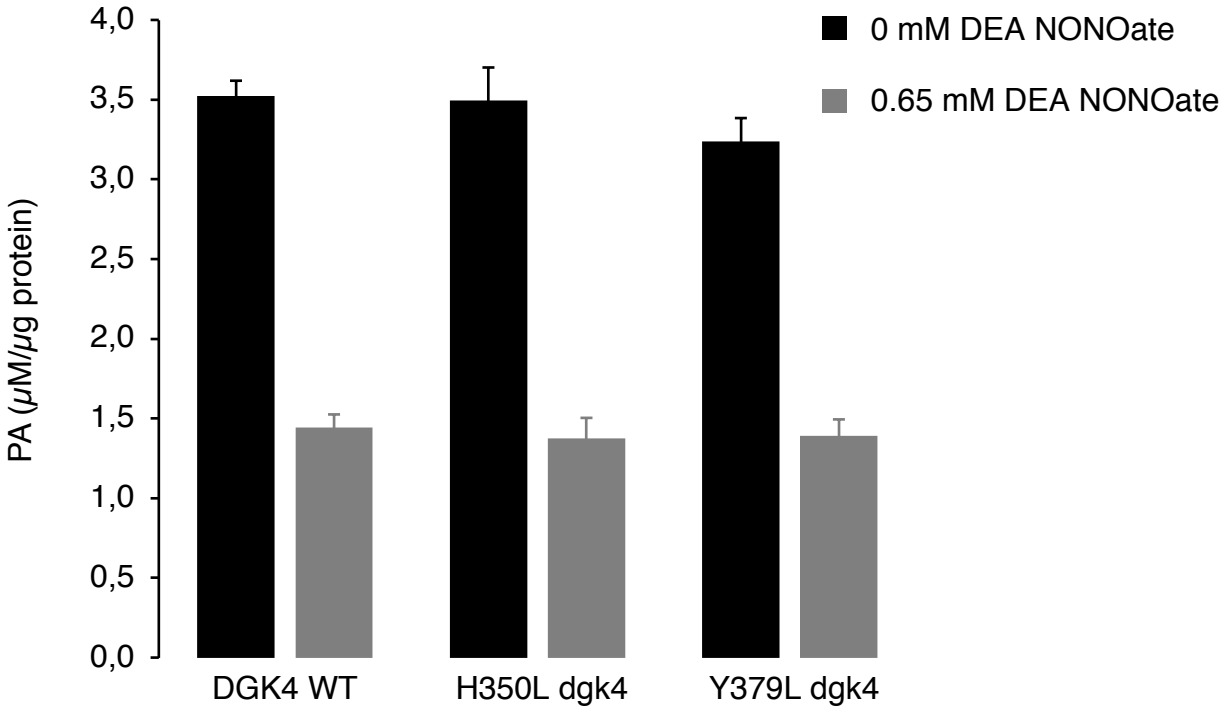

The kinase activities of dgk4 mutants H350L and Y379L were unaffected by the point mutations at the H-NOX-like center and were inhibited by NO to comparable degree as the WT. Kinase assay was done in reaction mixtures containing 40 mM Bis-Tris (pH 7.5), 5 mM $MgCl_2$, 0.1 mM EDTA, 1 mM spermine, 0.5 mM dithiothreitol, 1 mM sodium deoxycholate, 0.02% (v/v) Triton X-100, 500 μM 1,2-DOG and 1 mM ATP, with or without 0.65 mM DEA NONOate (see Materials and Methods for details). Black solid bars represent kinase reactions performed in the absence of NO while grey solid bars represent kinase reactions performed in the presence of NO (n = 6).

Table S1. UV-Vis spectroscopic data of selected heme proteins

	Soret / β / α ; max. absorption / nm			Source
Protein (*sp.*)	ferric	ferrous	ferrous-NO	
DGK4 (*At*)	410 / α + β 534	424 / 526 / 558	418 / - / -	This work
H-NOX (*So*)	403 / - / -	430 / α + β 560	399 / 543 / 572	Herzik et al., 2014
Cyt b5 (*Gl*)	411 / α + β 532	423 / 526 / 558		Alam et al., 2012
Z-ISO (*At*)	414 / α + β 531	414 / 529 / 559		Beltran et al., 2015

Legend: *At*: *Arabidopsis thaliana, So: Shiwanella oneidensis, Gl: Giardia lamblia.*

Table S2. Primers for *DGK4* and characterization of *dgk4-1* and *dgk4-2* plants

Primer name	Sequence (5' – 3')
***DGK4* cloning**	
DGK4 F	ATGGAATCACCGTCGATTGG
DGK4 R	TCAATCTCCTTTGACGACCAA
DGK4 H-L F	TTATGACATTGCTTATAAAAAAGTTGG
DGK4 H-L R	CAACTTTTTTATAAGCAATGTCATAAA
DGK4 Y-L F	ATCTACATAGCTTAGGAAGTGGAAGAA
DGK4 Y-L R	TCTTCCACTTCCTAAGCTATGTAGATT
Screening for homozygous *dgk4-1* and *dgk4-2* plants	
DGK4 promoter forward	TGTTTCTGACATCTGAGAACTTTT
DGK4 reverse	GATTGCATTCTTCGTAAAGACG
T-DNA	GTTCACGTAGTGGGCCATCG
Expression of *DGK4*	
DGK4 qPCR forward	CGTCGATTGGTGATTCATTG
DGK4 qPCR reverse	TTGCAATGCGGAGATATTGA
PP2AA3 qPCR forward	GCGGTTGTGGAGAACATGATACG
PP2AA3 qPCR reverse	GAACCAAACACAATTCGTTGCTG

Note: The underlined nucleotides incorporate the mutations changing histidine or tyrosine residues at positions 350 and 379 to leucine.

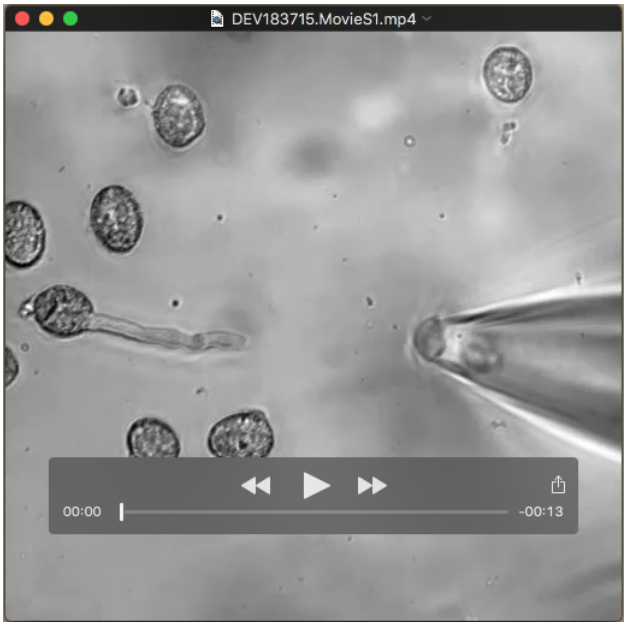

Movie 1

PT re-orientation responses of Col-0 to NO

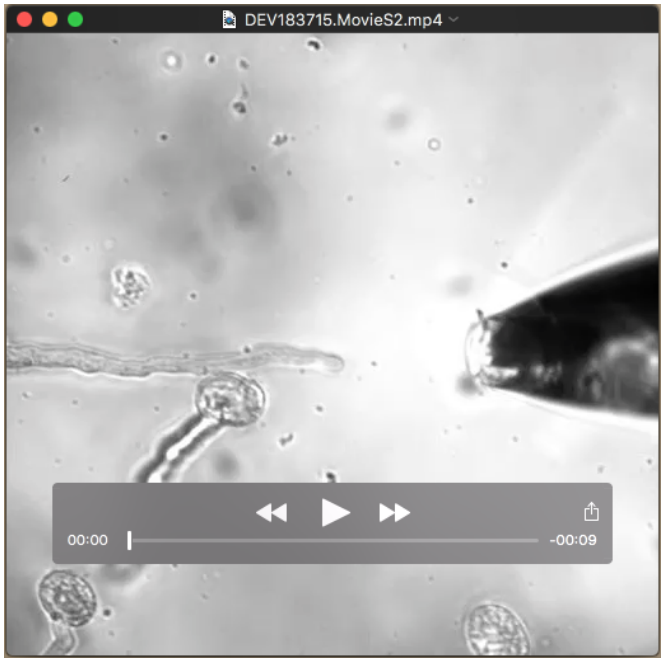

Movie 2

PT re-orientation responses of *dgk4-1* to NO

Supplementary references

1. Prado, A. M., Colaco, R., Moreno, N., Silva, A. C. and Feijo, J.A. (2008). Targeting of pollen tubes to ovules is dependent on nitric oxide (NO) signaling. *Mol. Plant* **1**, 703-714.
2. Prado, A. M., Porterfield, D. M. and Feijo, J.A. (2004). Nitric oxide is involved in growth regulation and re-orientation of pollen tubes. *Development* **131**, 2707-2714.
3. Meijering, E., Jacob, M., Sarria, J. C., Steiner, P., Hirling, H. and Unser, M. (2004). Design and validation of a tool for neurite tracing and analysis in fluorescence microscopy images. *Cytometry A* **58**, 167-176.
4. Herzik, M. A., Jonnalagadda, R., Kuriyan, J. and Marletta, M. A. (2014). Structural insights into the role of iron–histidine bond cleavage in nitric oxide-induced activation of H-NOX gas sensor proteins. *Proc. Natl. Acad. Sci. U.S.A.* **111**, E4156-E4164.
5. Alam, S., Yee, J., Couture, M., Takayama, S. J., Tseng, W. H., Mauk, A. G. and Rafferty, S. (2012). Cytochrome b5 from Giardia lamblia. *Metallomics* **4**, 1255-1261.
6. Beltran, J., Kloss, B., Hosler, J. P., Geng, J., Liu, A., Modi, A., Dawson, J. H., Sono, M., Shumskaya, M., Ampomah-Dwamena, C. et al. (2015). Control of carotenoid biosynthesis through a heme-based cis-trans isomerase. *Nat. Chem. Biol.* **11**, 598-605.